Tunneling and thermoelectric effect in generalized tunnel junctions in the presence of electron-hole asymmetry

J. E. Hirsch
Department of Physics, University of California, San Diego, La Jolla, California 92093-0319
(Received 2 March 1994)

The analysis of Blonder, Tinkham, and Klapwijk describing the crossover between tunnel junction and metallic contact between a normal and a superconductive electrode is applied to the case of a superconductor with an energy-dependent gap function. Such energy dependence arises in the presence of electron-hole asymmetry and is predicted within the theory of hole superconductivity. We study a tight-binding model where the interface is described by a reduced value of the intersite hopping amplitude and the superconducting gap function has on-site and nearest-neighbor components. The tunneling conductance as function of barrier strength is found to exhibit certain differences with the electron-hole symmetric case: the reflection and transmission coefficients are different for incident electrons and holes, and Andreev reflection processes for both electrons and holes are suppressed even in the limit of vanishing barrier strength. A temperature gradient across the barrier gives rise to a thermoelectric effect of universal sign, whose magnitude depends on the degree of electron-hole asymmetry in the superconductor as well as on the barrier strength. For temperatures close to T_c an analytic form for the thermoelectric voltage for arbitrary barrier strength is found. These results give information on the effect of nonideal tunnel barriers on the predicted thermoelectric effect. The possibility of observing these effects in high-temperature and conventional superconductors, and interpretation of existing experimental findings in light of these results is discussed.

I. INTRODUCTION

Tunneling into superconductors has proven to be a powerful tool to gain information on the nature of the superconducting state, and has also found a variety of practical applications.[1] The simplest analysis of tunneling processes,[2] using a "tunneling Hamiltonian,"[3] assumes an "ideal tunnel barrier," a uniform insulating layer between metallic electrodes. However, in practice any barrier will have some degree of nonuniformity, with regions of smaller resistance and in some cases even allow for metallic contact between the electrodes. Thus it is important to understand the effect of varying barrier strength on the tunneling process. In a seminal paper, Blonder, Tinkham, and Klapwijk[4] introduced and analyzed a one-dimensional model that interpolates between an ideal tunnel junction and a metallic contact as the strength of the scattering potential at the interface decreases. The model was shown to reproduce a variety of tunneling characteristics observed in Cu-Nb point-contact junctions.[5]

The treatment of Blonder *et al.* assumed a continuum model and a δ-function scattering potential at the interface between the normal metal and the superconductor; it also assumed an energy-independent BCS gap. Here we study instead a tight-binding model, where the interactions in the model of hole superconductivity are defined.[6,7] For a barrier defined by a different on-site energy at the boundary site between metal and superconductor, and an interaction that is only on site (attractive Hubbard model), the results for the tight-binding model and the continuum model of Blonder *et al.* are seen to be identical. An alternative way to represent the barrier in the tight-binding model is through a different hopping amplitude between neighboring sites across the interface. As the magnitude of this hopping amplitude decreases from its bulk value to zero the strength of the barrier increases from zero to infinity. For the case of an energy-independent gap as in the attractive Hubbard model the results for this case are similar but not identical to those of Blonder *et al.*

In this paper we assume a linear energy-dependent BCS gap function in the superconducting side, as arises in the model of hole superconductivity.[6] The energy dependence originates in the electron-hole asymmetric nature of superconductors postulated within that model, which is expected to be particularly significant in high-T_c oxides. We have considered both the case of a barrier defined by a different on-site energy, and by a different near-neighbor hopping amplitude at the interface. The latter barrier is found to be simpler to analyze when electron-hole asymmetry exists and we will concentrate on it in this paper (the former one is briefly discussed in Appendix B). Tunneling characteristics are found to exhibit an asymmetry of universal sign for a wide range of barrier strengths, similarly to what was found in the case of ideal tunnel barriers for this model.[8] Additionally, other differences with the conventional case of Blonder *et al.* are found. In particular, Andreev reflection processes are significantly suppressed compared to the case studied by Blonder *et al.*.

Furthermore we examine the situation where the quasi-

particles in the superconducting and normal electrodes are described by different distribution functions. Such a situation can be achieved by irradiating one side of the tunnel junction by electromagnetic radiation,[9,10] or by Joule heating techniques,[11] resulting in a temperature gradient across the barrier. For the case of an ideal tunnel junction it was recently found that a thermoelectric effect of universal sign is expected within the model of hole superconductivity.[12] This effect gives direct information on the magnitude of a fundamental parameter of the theory, ν, that measures the importance of electron-hole asymmetry in the superconductor. It is of interest to determine how this effect can be modified if the barrier is nonideal. We find that the magnitude of the effect is reduced as the strength of the barrier decreases and nearly vanishes for a metallic contact. The dependence on barrier strength is also a strong function of temperature. However, the sign remains universal and the magnitude is appreciable for a wide range of parameters so that the effect should be readily observable.

In Sec. II we discuss the formalism, Sec. III presents results for probability currents and tunneling characteristics in the absence of temperature gradients, and Sec. IV examines the thermoelectric effect as a function of barrier strength. Section V gives a more complete discussion of the thermoelectric effect in the ideal tunnel barrier case given in Ref. 12. In Sec. VI we examine the dependence of the fundamental asymmetry parameter ν on the microscopic interactions in the Hamiltonian, and we conclude in Sec. VII with a discussion.

II. FORMALISM

We consider a one-dimensional tight-binding model with kinetic energy,

$$H_0 = -\sum_{i\sigma} t_{i,i-1}(c^\dagger_{i\sigma}c_{i-1,\sigma} + \text{H.c.}) - \mu\sum_{i\sigma} c^\dagger_{i\sigma}c_{i\sigma} \ , \quad \text{(1a)}$$

$$t_{i,i-1} = t(1-\delta_{i,0}) + t'\delta_{i,0} \ . \quad \text{(1b)}$$

Here, $c^\dagger_{i\sigma}$ creates a hole of spin σ at site i, and μ is the hole chemical potential. The problem can of course equally well be formulated in the electron representation but we choose the hole representation here for consistency with our previous work. The hopping amplitude between neighboring sites is t except for hopping between sites -1 and 0 where it is t'. The barrier is thus characterized by the dimensionless parameter $\tau = t'/t$, with $0 \le \tau \le 1$. As $\tau \to 1$ it becomes a normal metallic contact while for $\tau \to 0$ it should describe an ideal tunnel junction.

Within the Bogoliubov formalism the equations of motion in the superconducting or normal state can be written as a two-dimensional matrix equation[13]

$$H\Psi = E\Psi \ , \quad (2)$$

where the two-component wave function is

$$\Psi = \begin{pmatrix} \Psi_1 \\ \Psi_2 \end{pmatrix} \quad (3)$$

and the Hamiltonian is

$$H = \begin{pmatrix} H_0 & \Delta \\ \Delta & -H_0 \end{pmatrix} \ . \quad (4)$$

The two entries in Eq. (3), Ψ_α, are vectors in position space with value $\Psi_\alpha(i)$ at lattice site i. The entries in the matrix Eq. (4) are matrices in position space: H_0 is the first-quantized version of Eq. (1), and the gap Δ has on-site and nearest-neighbor components in the model of hole superconductivity:

$$(\Delta)_{ij} = \Delta_{00}\delta_{ij} + \Delta_{01}(\delta_{j,i+1} + \delta_{j,i-1}) \ . \quad (5)$$

For a uniform superconductor, the gap function in momentum space is given by

$$\Delta_k = \sum_j e^{ik(R_j - R_i)}(\Delta)_{ij} = \Delta_m\left[\frac{-\epsilon_k}{D/2} + c\right] \equiv \Delta(\epsilon_k) \ , \quad (6)$$

with $D = 2zt$ the bandwidth (z = number of nearest neighbors to a site= 2 in the present case), $\epsilon_k = -2t\cos k$ the band energy, and Δ_m and c parameters obtained from solution of the BCS equations.[6] The real space gap components in this case are

$$\Delta_{00} = \Delta_m c \ , \quad \text{(7a)}$$

$$\Delta_{01} = \frac{\Delta_m}{z} \ . \quad \text{(7b)}$$

To properly deal with a nonhomogeneous situation one should solve the Bogoliubov equations self-consistently to find values of the gap parameters Δ_{00} and Δ_{01} at every lattice site and bond, which should approach the "bulk values" Eq. (7) sufficiently far away from the inhomogeneous region.[14] For the interface problem of interest here however we adopt a simplified procedure, following the treatment of Blonder *et al.* al. We assume the system is a normal metal for $i < 0$ with gap values

$$(\Delta)_{ii} = (\Delta)_{i,i+1} = (\Delta)_{i+1,i} = 0, \quad (8)$$

and a superconductor for $i \ge 0$ with gap values

$$(\Delta)_{ii} = \Delta_{00} \ , \quad (9)$$

$$(\Delta)_{i,i+1} = (\Delta)_{i+1,1} = \Delta_{01} \ , \quad (10)$$

independent of i, and solve the scattering problem for a particle incident on the barrier. The incident, transmitted, and reflected waves for a hole coming in from the left are of the same form as in Blonder *et al.*:

$$\Psi_{\text{in}}(i) = \begin{pmatrix} 1 \\ 0 \end{pmatrix} e^{iq^+R_i} \ , \quad \text{(11a)}$$

$$\Psi_{\text{re}}(i) = a\begin{pmatrix} 0 \\ 1 \end{pmatrix} e^{iq^-R_i} + b\begin{pmatrix} 1 \\ 0 \end{pmatrix} e^{-iq^+R_i} \ , \quad \text{(11b)}$$

$$\Psi_{\text{tr}}(i) = c\begin{pmatrix} u \\ v \end{pmatrix} e^{ik^+R_i} + d\begin{pmatrix} u' \\ v' \end{pmatrix} e^{-ik^-R_i} \ , \quad \text{(11c)}$$

where b gives the amplitude for ordinary reflection, a is the amplitude for Andreev reflection, and c and d are amplitudes for transmission on the same side and opposite side of the Fermi surface respectively. The relation between wave vectors and the quasiparticle energy E is

$$\epsilon_{q^+} - \mu = \mu - \epsilon_{q^-} = E \ , \tag{12a}$$

$$\epsilon_{k^+} - \mu = \nu + \frac{1}{a_0}\sqrt{E^2 - \Delta_0^2} \ , \tag{12b}$$

$$\epsilon_{k^-} - \mu = \nu - \frac{1}{a_0}\sqrt{E^2 - \Delta_0^2} \ , \tag{12c}$$

with

$$\Delta_0 = \frac{\Delta(\mu)}{a_0} \ , \tag{13a}$$

$$\delta = \frac{\Delta_m}{(D/2)} \ , \tag{13b}$$

$$\nu = \frac{\delta}{a_0}\Delta_0 \ , \tag{13c}$$

$$a_0 = \sqrt{1+\delta^2} \ . \tag{13d}$$

The BCS coherence factors are given by

$$u^2 = \frac{1}{2}\left(1 + \frac{\epsilon_{k^+} - \mu}{E}\right) \ , \tag{14a}$$

$$v^2 = \frac{1}{2}\left(1 - \frac{\epsilon_{k^+} - \mu}{E}\right) \ , \tag{14b}$$

$$u'^2 = \frac{1}{2}\left(1 + \frac{\epsilon_{k^-} - \mu}{E}\right) \ , \tag{14c}$$

$$v'^2 = \frac{1}{2}\left(1 - \frac{\epsilon_{k^-} - \mu}{E}\right) \ . \tag{14d}$$

Various useful relations between these coherence factors are given in Appendix A. In the electron-hole symmetric case considered by Blonder *et al.* $u' = v$, $v' = u$, and $\nu = \delta = 0$.

The wave function to the left of the interface, in the normal metal, is the sum of incident and reflected wave functions,

$$\Psi_L(i) = \Psi_I(i) + \Psi_{\rm re}(i), \tag{15}$$

and satisfies the Bogoliubov equations for $i < -1$. The wave function to the right of the interface, in the superconductor, is the transmitted wave

$$\Psi_R(i) = \Psi_{\rm tr}(i) \tag{16}$$

and satisfies the Bogoliubov equations for $i > 0$. The coefficients a, b, c, d are determined by the requirement that the wave functions satisfy the Bogoliubov equations

$$(H\Psi)_i = E\Psi(i) \tag{17}$$

at sites $i = -1$ and $i = 0$, yielding the equations

$$t\Psi_{1L}(0) - t'\Psi_{1R}(0) = 0 \ , \tag{18a}$$

$$-t\Psi_{2L}(0) + t'\Psi_{2R}(0) = 0 \tag{18b}$$

and

$$t\Psi_{1R}(-1) - t'\Psi_{1L}(-1) - \Delta_{01}\Psi_{2R}(-1) = 0 \ , \tag{19a}$$

$$-t\Psi_{2R}(-1) + t'\Psi_{2L}(-1) - \Delta_{01}\Psi_{1R}(-1) = 0 \ , \tag{19b}$$

respectively. Equation (18) yield the conditions

$$b = -1 + \tau(cu + du') \ , \tag{20a}$$

$$a = \tau(cv + dv') \ , \tag{20b}$$

and from Eqs. (19) and (20), approximating all wave vectors by the Fermi wave vector (k_F) one obtains for c and d the equations

$$a_{11}c + a_{12}d = c_1 \ , \tag{21a}$$

$$a_{21}c + a_{22}d = 0 \ , \tag{21b}$$

with

$$a_{11} = u(e^{-ik_F} - \tau^2 e^{ik_F}) - v\delta e^{-ik_F} \ , \tag{22a}$$

$$a_{12} = \left[u'(1-\tau^2) - v'\delta\right] e^{ik_F} \ , \tag{22b}$$

$$a_{21} = \left[-u\delta + v(\tau^2 - 1)\right] e^{-ik_F} \ , \tag{22c}$$

$$a_{22} = v'(-e^{ik_F} + \tau^2 e^{-ik_F}) - u'\delta e^{ik_F} \ , \tag{22d}$$

which are readily solved for c and d, and substituting in Eq. (20) the values of a and b are obtained. The result is

$$a = 2i\tau^2 \sin^2 k_F[-\delta r(uv' - u'v) + \delta(uv' + u'v) + 2ivv']/\gamma \ , \tag{23a}$$

$$b = -1 - 2\tau^2 \sin^2 k_F[2uu'\delta + (uv' - u'v)\{\tau^2 - ir(1-\tau^2)\} + uv' + u'v]/\gamma \ , \tag{23b}$$

$$c = 2i\tau \sin k_F[u'\delta e^{ik_F} + v'(e^{ik_F} - \tau^2 e^{-ik_F})]/\gamma \ , \tag{23c}$$

$$d = -2i \sin k_F[u\delta + v(1-\tau^2)]e^{-ik_F}/\gamma \ , \tag{23d}$$

$$\gamma = -(uv' - u'v)((1-\tau^2)^2 + \delta^2) - 4\tau^2 \sin^2 k_F \times \left[uv' + \frac{\delta}{2}(uu' - vv') - \frac{i\delta r}{2}(uu' + vv')\right] , \quad (23e)$$

$$r = \frac{\cos k_F}{\sin k_F} . \quad (23f)$$

For the electron-hole symmetric case ($\delta = 0$) these results are similar although not identical to the case considered by Blonder *et al.*

The wave functions Eq. (11) describe a hole coming in from the left, in the hole representation used here. For an *electron* coming in from the left the appropiate wave functions are:

$$\bar{\Psi}_{\rm in}(i) = \begin{pmatrix} 0 \\ 1 \end{pmatrix} e^{-iq^- R_i} , \quad (24a)$$

$$\bar{\Psi}_{\rm re}(i) = \bar{b}\begin{pmatrix} 0 \\ 1 \end{pmatrix} e^{iq^- R_i} + \bar{a}\begin{pmatrix} 1 \\ 0 \end{pmatrix} e^{-iq^+ R_i} , \quad (24b)$$

$$\bar{\Psi}_{\rm tr}(i) = \bar{d}\begin{pmatrix} u \\ v \end{pmatrix} e^{ik^+ R_i} + \bar{c}\begin{pmatrix} u' \\ v' \end{pmatrix} e^{-ik^- R_i} . \quad (24c)$$

The amplitudes $\bar{a}$, $\bar{b}$, $\bar{c}$, $\bar{d}$ satisfy equations identical to Eq. (23) with the substitution

$$\delta \to -\delta , \quad (25a)$$

$$k_F \to -k_F \quad (25b)$$

(with the substitution $\delta \to -\delta$ also in the coherence factors).

The probability currents for the case of incident holes from the normal metal are given by

$$A = |\, a \,|^2 , \quad (26a)$$

$$B = |\, b \,|^2 , \quad (26b)$$

$$C = \left[|\, u \,|^2 - |\, v \,|^2 - \delta\,(uv^* + u^* v)\right] |\, c \,|^2 , \quad (26c)$$

$$D = \left[|\, v' \,|^2 - |\, u' \,|^2 - \delta\,(u'v'^* + u'^* v')\right] |\, d \,|^2 , \quad (26d)$$

and similar expressions hold for the case of incident electrons, with the amplitudes given in the wave function Eq. (24). Note the extra terms in the transmitted currents C and D compared to the electron-hole symmetric case,[4] due to the fact that the off-diagonal components of the gap give a contribution to the current. They can be derived from the expression for the quasiparticle velocity

$$v_k = \frac{\partial E}{\partial \epsilon_k} \quad (27)$$

or from the continuity equation for the probability density that follows from the Bogoliubov equations. Some algebra verifies that the conservation of probability condition

$$A + B + C + D = 1 \quad (28)$$

follows from Eqs. (23) and (26), for $E > \Delta_0$. For $E < \Delta_0$,

$$A + B = 1 \quad (29)$$

holds, as in that case no quasiparticles can be transmitted into the superconducting side.

From the probability currents it is straightforward to calculate the quasiparticle current through the interface in the presence of an applied voltage V.[4] We assume that particles to the left and right of the barrier obey Fermi distribution functions $f_n(E)$ and $f_s(E)$ respectively, allowing for the possibility of different temperatures T_n and T_s in the normal and superconducting sides. The result for the (hole) current from the normal metal to the superconductor is

$$I_{\rm NS} = \frac{1+Z^2}{eR}\int_0^\infty dE\{[1 - B(E) + A(E)] \times [f_n(E - eV) - f_s(E)] + [1 - \bar{B}(E) + \bar{A}(E)] \times [f_s(E) - f_n(E + eV)]\} , \quad (30)$$

with V the voltage of the normal side relative to the superconducting side, R the resistance of the junction in the normal state, and Z the "effective barrier strength" defined by

$$Z = \frac{1-\tau^2}{2\tau \sin k_F} . \quad (31)$$

The transmission coefficient for this barrier when both sides are normal is $1/(1+Z^2)$, and the reflection coefficient is $Z^2/(1+Z^2)$.

It is important to verify that our results for the current Eq. (30) approach the results obtained from the tunneling Hamiltonian analysis as the strength of the barrier becomes large. For small τ the Andreev probability current A is proportional to τ^4 and can be neglected. The reflection probability current B for $E > \Delta_0$ is found to be

$$B = 1 - \frac{4\tau^2 \sin^2 k_F}{(1+\delta^2)(uv' - u'v)}[uv' + u'v + 2\delta uu'] \quad (32)$$

and using the relations in Appendix A we find

$$B = 1 - \frac{1}{a_0 Z^2}\frac{E}{\sqrt{E^2 - \Delta_0^2}}\left(1 + \frac{\nu}{E}\right) \quad (33)$$

and similarly $\bar{B}$ is given by Eq. (33) with ν replaced by $-\nu$. For $E < \Delta_0$ one can see from Eq. (29) that $1 - B \propto \tau^4$ so that this region gives negligible contribution to the current, and Eq. (30) becomes

$$I_{\rm NS} = \frac{1+Z^2}{eRa_0 Z^2}\int_{\Delta_0}^\infty dE \frac{E}{\sqrt{E^2 - \Delta_0^2}} \times \left[\left(1 + \frac{\nu}{E}\right)[f_n(E - eV) - f_s(E)] + \left(1 - \frac{\nu}{E}\right)[f_s(E) - f_n(E + eV)]\right] , \quad (34)$$

which is the result obtained from the tunneling Hamiltonian for large Z.[15]

In fact it is easy to see that the Andreev reflection probability is the same for an incident hole and electron at the same energy:

$$A(E) = \bar{A}(E) \tag{35}$$

for all energies. Equations (35) and (29) then imply that

$$B(E) = \bar{B}(E) \tag{36}$$

for $E < \Delta_0$, so that electron-hole asymmetry manifests itself only in the ordinary reflection and transmission probabilities for incident quasiparticles with energies above the superconducting gap. In particular the zero voltage thermoelectric current when the normal metal and the superconductor are at different temperatures is given by

$$I_0 = \frac{1+Z^2}{eR}\int_{\Delta_0}^{\infty} dE[\bar{B}(E) - B(E)][f_n(E) - f_s(E)] \; ; \tag{37}$$

that is, it originates in the different reflection probability for electrons and holes with $E > \Delta_0$. Although even for zero barrier ($\tau = 1$) are B and $\bar{B}$ slightly different it is only for large barrier that the thermoelectric effect becomes appreciable as will be seen in what follows.

III. PROBABILITY CURRENTS AND *I-V* CHARACTERISTICS

The importance of electron-hole symmetry breaking in the model of hole superconductivity is measured by the ratio ν/Δ_0, or equivalently the gap slope δ, given by Eq. (13b) or

$$\delta = \frac{\nu}{\sqrt{\Delta_0^2 - \nu^2}} \; . \tag{38}$$

Figure 1 shows the quasiparticle energy, gap function, and coherence factors versus band energy for $\delta = 0.4$ as an example. Note in particular that u^2 and v^2 are not equal at the minimum quasiparticle energy.

Figure 2 shows the probability currents for various barrier strengths for the case $\delta = 0.1$ and Fig. 3 for the case $\delta = 0.4$. We plot the probability currents for both incident holes and electrons, which are different for $E > \Delta_0$ (except for A): The reflection probability current B is larger for electrons than for holes, and the transmission probability currents C and D are smaller. The differences in magnitude increase as the gap slope increases and are largest for intermediate values of τ.

It can be seen that increasing δ suppresses the Andreev probability current A. For the case of no barrier ($\tau = 1$) one has in the electron-hole symmetric (EHS) case of Blonder *et al.* $A = 1$, $B = 0$ for $E < \Delta_0$ and $B = D = 0$ for $E > \Delta_0$. Here we find instead that $A < 1$ and $B > 0$ for both $E < \Delta_0$ and $E > \Delta_0$. As δ increases there

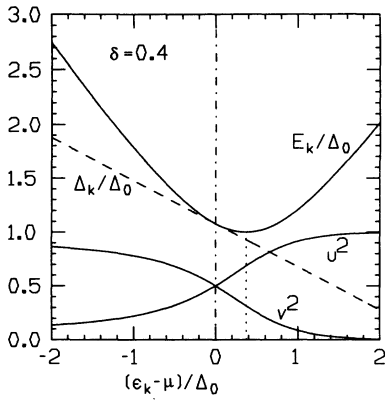

FIG. 1. Quasiparticle energy, gap function, and coherence factors versus hole band energy for gap slope $\delta = 0.4$. The vertical dot-dashed and dotted lines indicate the positions of the chemical potential μ and of the band energy giving rise to the minimum quasiparticle energy $\mu + \nu$.

is increasing ordinary reflection at low energies. Also for $E > \Delta_0$ we find here that there is also a finite probability current for scattering across the Fermi surface ($D \neq 0$) even for vanishing barrier strength.

These effects cannot be represented by an "effective barrier strength"[5] in the EHS model: For $E = \Delta_0$ we find for the Andreev probability current

$$A = \frac{1}{1 + \frac{\delta^2}{\sin^2 k_F}} \; , \tag{39}$$

independent of barrier strength, so that $A < 1$, $B > 0$ if $\delta \neq 0$. In contrast in the EHS case $A = 1$, $B = 0$ at $E = \Delta_0$ independent of barrier strength.[4]

As the barrier strength is increased (τ is reduced from unity) the effect is qualitatively similar to what is found in the EHS case: A is reduced and B is enhanced both for $E < \Delta_0$ and $E > \Delta_0$. Although A generally increases with energy for $E < \Delta_0$ its maximum does not always occur exactly at $E = \Delta_0$. This can be seen for example in Fig. 3(c) where the maximum A occurs for E slightly smaller than Δ_0 and is larger than the value given by Eq. (39).

It is also interesting to examine the effect of carrier density on the probability currents. The carrier density determines the Fermi wave vector k_F in the amplitudes Eq. (23) as well as the effective barrier strength Eq. (31). We assume a two-dimensional system where for low density of carriers n the Fermi wave vector is given by

$$k_F = \sqrt{2\pi n} \; , \tag{40}$$

so that the effective barrier strength Eq. (31) increases as the density decreases. The asymmetry parameter δ also depends on density in our model.[6] Beyond these effects however there is an additional dependence of the probability currents on density, as shown in Fig. 4 for the case $\tau = 1$: As the carrier density decreases the effect of electron-hole asymmetry becomes more important.

Tunneling characteristics resulting from these proba-

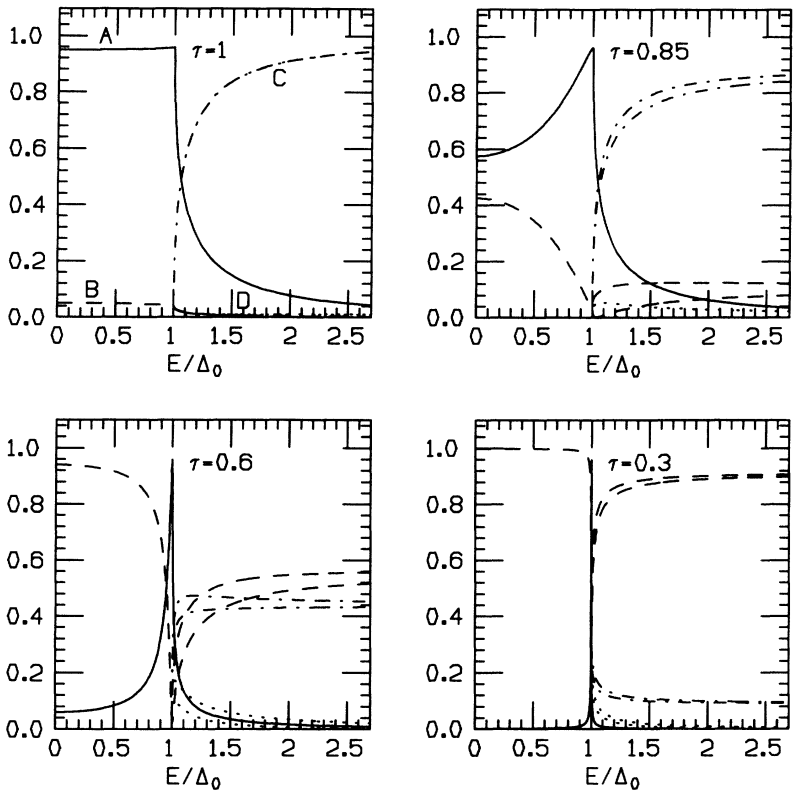

FIG. 2. Probability currents for gap slope $\delta = 0.1$ for various barrier strengths τ (indicated in the figure). Solid, dashed, dot-dashed, and dotted lines correspond to Andreev reflection (A), ordinary reflection (B), and transmission on the same side (C) and on opposite sides (D) of the Fermi surface respectively. Probability currents for both incident holes and electrons, which are different (except for A) for $E > \Delta_0$, are plotted with the same line convention: B is larger for electrons than for holes, and C and D are smaller. In this and following figures hole density is $n = 0.04$ except when explicitely indicated otherwise.

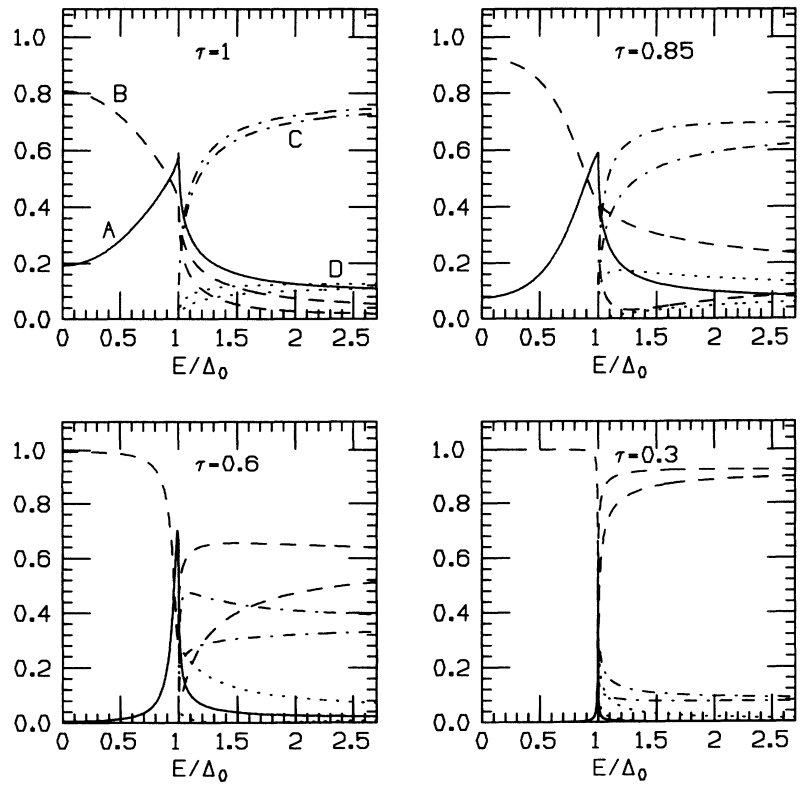

FIG. 3. Same as Fig. 2 for gap slope $\delta = 0.4$.

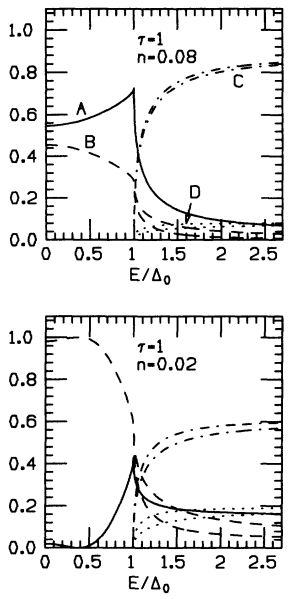

FIG. 4. Probability currents for gap slope $\delta = 0.4$, $\tau = 1$, and two values of the hole density.

bility currents are shown in Figs. 5 and 6 for low temperatures. At zero temperature we have from Eq. (30)

$$I_{\rm NS} = \frac{1+Z^2}{eR}[1 - B(eV) + A(eV)], \quad V > 0 , \tag{41a}$$

$$I_{\rm NS} = \frac{1+Z^2}{eR}[1 - \bar{B}(-eV) + A(-eV)], \quad V < 0 . \tag{41b}$$

For the case of small asymmetry the results look qualitatively similar to those of Blonder *et al.*, with an enhanced conductance at low voltage when the barrier is weak (Fig. 5). For large asymmetry however even in the case of zero barrier the conductance is suppressed in the gap region as seen in Fig. 6. This is due to the fact that the ordinary reflection probability is larger than the Andreev reflection probability, as seen in Fig. 3. The qualitative behavior seen in Fig. 6 for $\tau = 1$, a decreased conductance at low voltage without an enhancement of conductance for voltages around the gap edge, is not seen in the EHS case for any value of the barrier strength. As the barrier strength increases the results approach the tunneling characteristics obtained from the tunneling Hamiltonian approach (dashed lines).

To look at the temperature dependence of tunneling characteristics it is necessary to know the temperature dependence of the gap Δ_0 and asymmetry parameter δ. For that purpose we choose interaction parameters in the model of hole superconductivity that yield gap and asymmetry parameters similar to the two representative cases of small and large asymmetry just discussed. The way these parameters enter in the microscopic Hamiltonian is reviewed in Sec. VI.

Case 1:

$$U = 5 \text{ eV} , \tag{42a}$$

$$K = 3.61 \text{ eV} , \tag{42b}$$

$$W = 2.24 \text{ eV} , \tag{42c}$$

$$D_h = 0.24 \text{ eV} , \tag{42d}$$

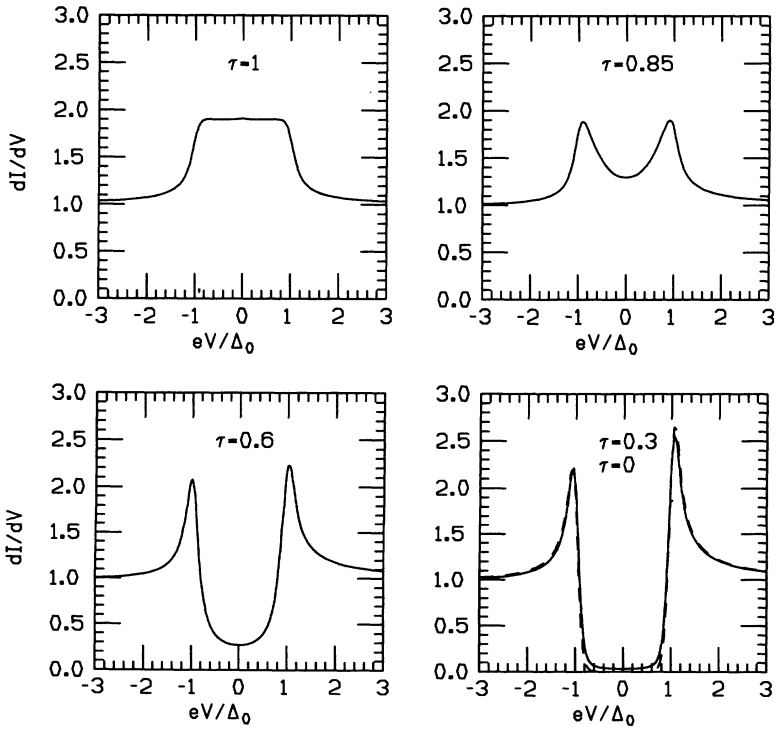

FIG. 5. Tunneling characteristics for various barrier strengths for gap slope $\delta = 0.1$. Here and in the following figures the resistance of the barrier when both electrodes are in the normal state is assumed to be 1 Ω. The dashed lines are the results for the ideal tunnel barrier ($\tau = 0$) obtained from the tunneling Hamiltonian approach. The sign of V refers to the polarity of the normal electrode.

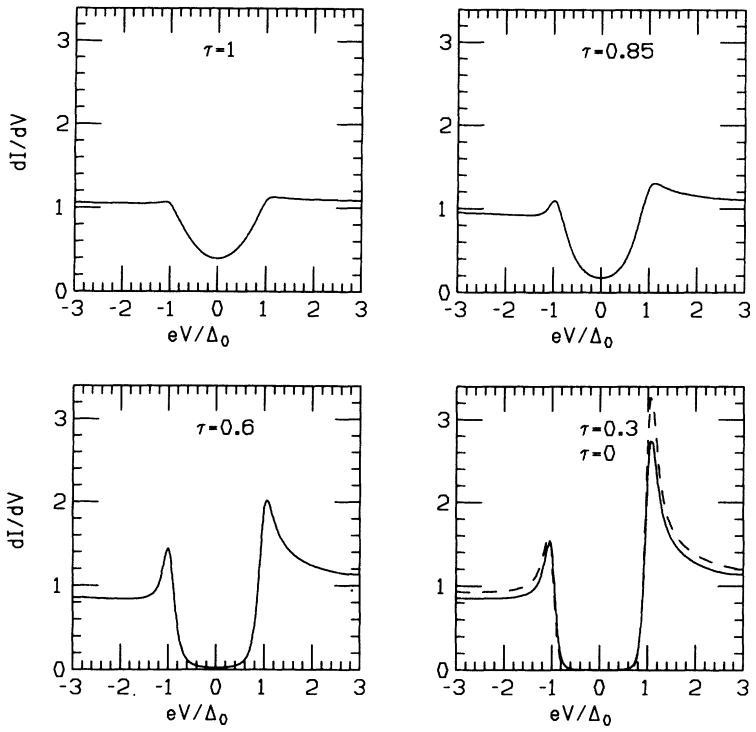

FIG. 6. Same as Fig. 5 for gap slope $\delta = 0.4$.

Case 2:

$$U = 5 \text{ eV} , \tag{43a}$$

$$K = 2.20 \text{ eV} , \tag{43b}$$

$$W = 0.73 \text{ eV} , \tag{43c}$$

$$D_h = 0 . \tag{43d}$$

For case 1 one has $T_c = 93.13$ K and $\Delta_0 = 15.6$ meV, $\delta = 0.107$ at low temperatures; for case 2, $T_c = 92.64$ K , $\Delta_0 = 18.2$ meV, $\delta = 0.397$. The gap slope δ decreases as the temperature increases and approaches zero as $T \to T_c$.

Figures 7 and 8 show tunneling characteristics for various barrier strengths and temperatures. For zero barrier the enhanced conductance at low voltages that occurs for weak asymmetry is not strongly temperature dependent; in contrast the reduced conductance that occurs for large asymmetry increases substantially as T increases. As the barrier height increases the effect of temperature in all cases is to suppress the peaks at voltages around the gap energy and increase the in-gap conductance. The asymmetry in dI/dV is appreciable in a range of barrier strengths and temperatures.

IV. THERMOELECTRIC EFFECT

The fact that probability currents for quasiparticles with energies larger than the superconducting gap are different for electrons and holes gives rise to a net charge current in the absence of an applied voltage when the quasiparticles in the normal and superconducting electrodes obey different distribution functions, as would occur in the presence of a temperature gradient across the junction. In this section we examine the effect of barrier strength on this thermoelectric effect.

Figure 9 shows current versus voltage for an ideal tunnel junction with the normal metal at 19 K and the superconductor at 20 K, for a case with gap $\Delta_0 = 15$ meV and gap slope $\delta = 0.4$. On amplifying the scale near the origin (inset) the thermoelectric effect becomes apparent: The I-V curve is displaced towards the negative I region in this case. Smaller gap slopes give smaller magnitude but otherwise similar effect. The effect of varying barrier strength for this case is shown in Fig. 10. On increasing τ from zero the zero current voltage is rapidly reduced, and the zero voltage current also decreases although more slowly. Note that for $\tau = 0.3$ where the tunneling characteristics are not very different from the ideal tunnel barrier case (Fig. 6) the zero current voltage is reduced here by about 85% from the ideal barrier case.

We next look in more detail at the effect of barrier strength and temperature on the zero current voltage V_t and the zero voltage current I_0. Figure 11(a) shows V_t versus τ for various temperatures, for the parameters of case 2 discussed in the previous section and $T_n = T_s - 1$ K. As the temperature increases the effect of barrier strength is seen to decrease. For low temperatures, V_t decreases very rapidly as τ increases. Figure 11(b) shows the zero voltage current. Here, the dependence on barrier strength is similar at all temperatures.

These results are relevant to interpret results of experiments within this model. Assume that for a given tem-

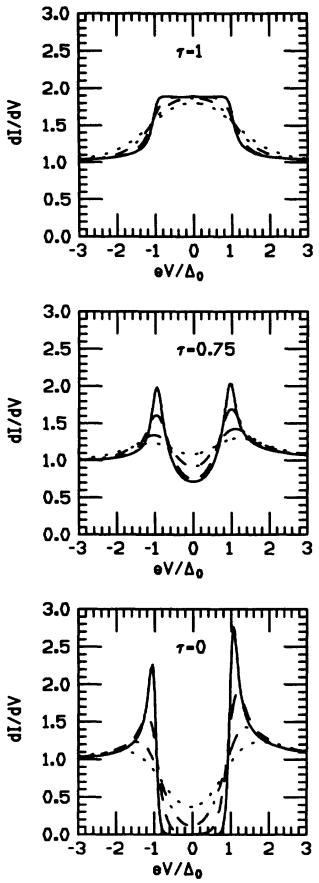

FIG. 7. Temperature dependence of tunneling characteristics for various barrier strengths. Parameters for case 1 in the text are used. The zero temperature gap slope and gap value are $\delta = 0.107$, $\Delta_0 = 15.63$ meV. $T_c = 93.13$ K. Solid, dashed, dot-dashed and dotted lines correspond to temperatures $T/T_c = 0.1$, 0.25, 0.5, and 0.7 respectively.

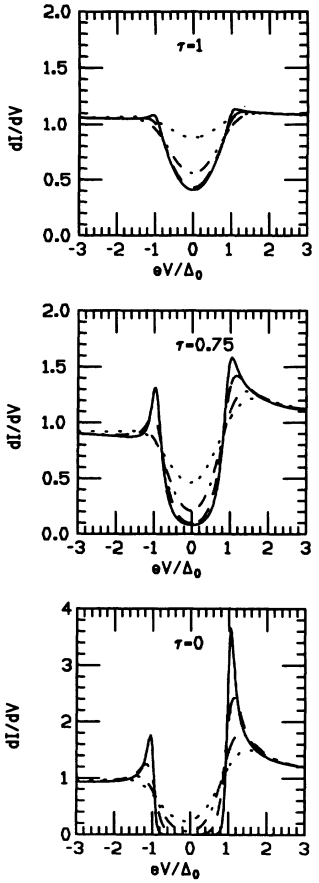

FIG. 8. Same as Fig. 7 for parameters of case 2 (see text). At zero temperature $\delta = 0.397$, $\Delta_0 = 18.23$ meV. $T_c = 92.37$ K.

perature difference between the normal metal and the superconductor, $\Delta T = T_n - T_s$, one observes a thermoelectric voltage that increases as T decreases below T_c but then decreases at lower temperatures. For a perfect barrier ($\tau = 0$) this would indicate that electron-hole asymmetry is becoming smaller as the temperature is lowered, which would be inconsistent with the model of hole superconductivity. Instead, for an imperfect barrier (τ finite) that is precisely what is expected within the model, as seen in Fig. 12(a). In the dI/dV characteristics instead there would be not much difference between a perfect and an imperfect barrier. The zero voltage current [Fig. 12(b)] does not differ qualitatively between perfect and imperfect barriers, going to zero exponentially at low temperatures in both cases. Note also in Fig. 12(b) that there is a finite thermoelectric current even for vanishing barrier strength ($\tau = 1$). The corresponding thermoelectric voltage is almost indistinguishable from zero on the scale of Fig.12(a).

For an ideal tunnel barrier it was shown in Ref. 12 that the zero current thermoelectric voltage is given by

$$V_t = \frac{\nu}{e}\frac{T_s - T_n}{T_n} , \qquad (44)$$

so that V_t gives direct information on the fundamental asymmetry parameter ν and on the gap slope δ given an independent estimate of the gap Δ_0. This relation is no longer valid for a generalized barrier. In Fig. 13 we plot the combination $(V_t T/\Delta T)$ for various barrier strengths and temperature gradients $\Delta T = T_n - T_s$, as well as ν

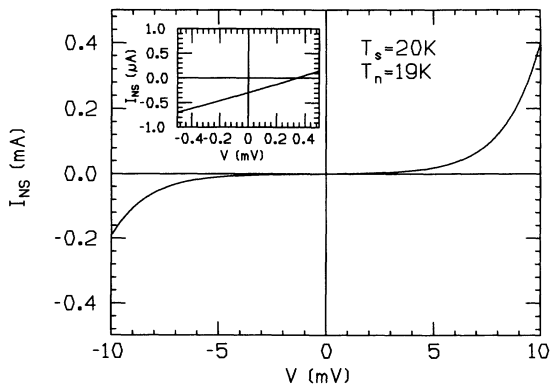

FIG. 9. Current versus voltage for ideal tunnel junction with normal electrode at 19 K and superconducting electrode at 20 K. Gap in superconductor is $\Delta_0 = 15$ meV and gap slope is $\delta = 0.4$. Inset shows data with amplified scale near the origin.

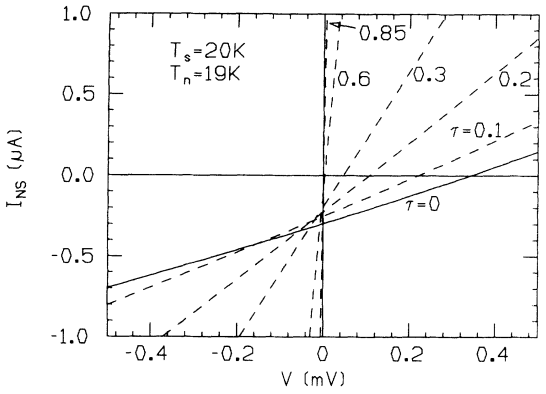

FIG. 10. Current versus voltage for the case of Fig. 9 for various barrier strengths (value of τ given next to each line). The ideal tunnel junction results are given by the solid line.

versus temperature. For $\tau = 0$ (ideal barrier) the results deviate from ν only due to the finiteness of ΔT. For $\tau \neq 0$ however the results go to zero as the temperature is lowered. For T close to T_c however it can be seen that the results for finite τ and for the ideal tunnel barrier are very similar.

It is in fact possible to obtain an analytic form for the thermoelectric voltage for general τ for temperatures close to T_c. Expansion of the Fermi functions in Eq. (30) for small voltage and temperature gradient yields

$$I_{\rm NS} = \frac{1+Z^2}{eR}\int_0^\infty dE\left(\frac{\partial f_n}{\partial E}\right)\left[[B(E)-\bar{B}(E)]\right.$$
$$\left.\times E\frac{(T_s-T_n)}{T_n} + eV[2-B(E)-\bar{B}(E)+2A(E)]\right] \tag{45}$$

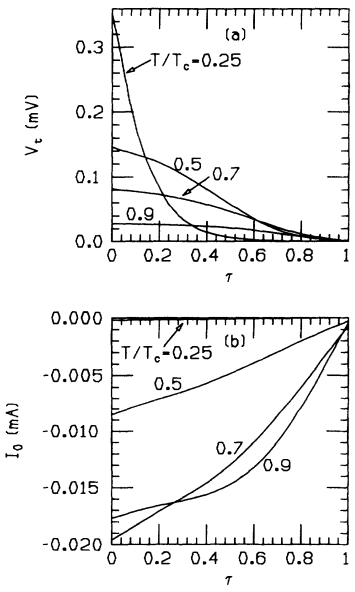

FIG. 11. (a) Zero current voltage and (b) zero voltage current for parameters of case 2 as function of barrier strength for various temperatures (given in the figure). The normal metal is 1 K colder than the superconductor.

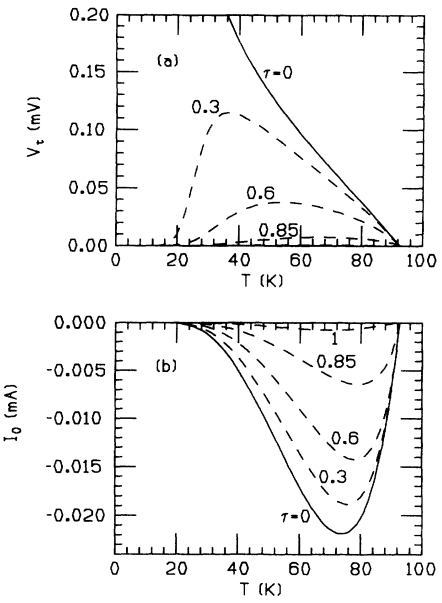

FIG. 12. (a) Zero current voltage and (b) zero voltage current versus temperature for parameters of case 2 for various barrier strengths τ (given in the figure). The temperature of the superconducting electrode is T and that of the normal metal is $T - 1$ K.

and setting the integrand to zero yields for the voltage

$$V = \frac{(\bar{B}-B)E}{e(2-B-\bar{B}+2A)}\frac{T_s-T_n}{T_n}\,. \tag{46}$$

The right hand side of Eq. (46) can be shown to be independent of energy in the region where $\delta \ll 1$ and $\Delta_0 \ll E < \Delta_0^2/\nu$. As $T \to T_c$ this region dominates the

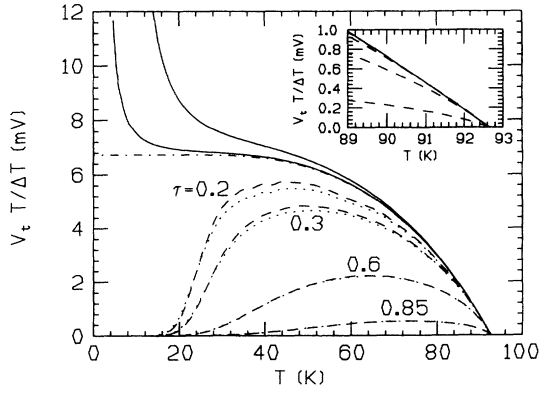

FIG. 13. Zero current voltage V_T times temperature divided by temperature difference ΔT between the superconductor and the normal metal. The dot-dashed line gives the asymmetry parameter ν. The two solid lines give results for the ideal tunnel barrier with temperature difference $\Delta T = 1$ K and 0.1 K; the lower solid line corresponds to the smaller ΔT. The dashed and dotted lines give results for the generalized barrier for $\Delta T = 1$ K and 0.1 K respectively for various barrier strengths (given in the figure). The inset (same line convention) gives results close to T_c for ν, for the ideal tunnel barrier and for $\tau = 0.3$, 0.6, and 0.85.

integral Eq. (45) and one finds for the thermoelectric voltage a generalized form of Eq. (44):

$$V_t = \frac{\nu(\tau, k_F)}{e} \frac{T_s - T_n}{T_n} , \tag{47}$$

with

$$\nu(\tau, k_F) = \frac{1-\tau^4}{(1-\tau^2)^2 + 4\tau^2 \sin^2 k_F} \nu , \tag{48}$$

so that the thermoelectric power for a generalized barrier is

$$S = \frac{\nu(\tau, k_F)}{eT} \tag{49}$$

for T close to T_c. Note in particular that S for finite τ can be larger than S for $\tau = 0$. The numerical results of Fig. 13 show good agreement with the form Eq. (48) for T close to T_c.

More generally, the thermoelectric power at any temperature can be written in the form Eq. (49), with

$$\nu(\tau, k_F) = \frac{\int_{\Delta_0}^{\infty} dE (\frac{\partial f_n}{\partial E})[\bar{B}(E) - B(E)]E}{\int_0^{\infty} dE (\frac{\partial f_n}{\partial E})[2 - B(E) - \bar{B}(E) + 2A(E)]} . \tag{50}$$

From this expression it is easy to see why the thermoelectric voltage goes to zero as T decreases when τ is finite. At low temperatures the region in energy close to Δ_0 dominates the integral in the numerator of Eq. (50), due to the Fermi function derivative; B and $\bar{B}$ are continuous functions of energy, and $[\bar{B}(E) - B(E)]$ approaches zero as $E \to \Delta_0$.

V. IDEAL TUNNEL BARRIER

In this section we expand on the discussion of the ideal tunnel barrier in the presence of electron-hole asymmetry given in Refs. 8 and 12. As usual we consider the two sides of the barrier as noninteracting systems and calculate the current using the "tunneling Hamiltonian" and second order perturbation theory.[2] The current is proportional to the square of a tunneling matrix element, assumed to be energy independent, and the density of final states.

The Bogoliubov relations between fermion and quasiparticle operators are as usual

$$c_{k\uparrow} = u_k \alpha_k + v_k^* \beta_k^\dagger , \tag{51a}$$

$$c_{-k\downarrow}^\dagger = -v_k \alpha_k + u_k^* \beta_k^\dagger . \tag{51b}$$

We use the representation where $c_{k\sigma}^\dagger$ creates a *hole* of spin σ. In that case the coherence factors are given by Eq. (14). Consider for definiteness the tunneling of a hole of spin up. The following processes can occur:

(1) Hole goes from normal metal to superconductor, and an excitation α_k of energy E_k is created in the superconductor. The probability for this to occur is $|u_k|^2$. By adding the contributions from the two momentum states giving rise to the same quasiparticle energy [Eq. (14)],

$$|u_k|^2 + |u_k'|^2 = 1 + \frac{\nu}{E_k} , \tag{52}$$

the contribution to the current from the normal metal (N) to the superconductor (S) is proportional to

$$J_{\rm NS}^{(1)} = \left(1 + \frac{\nu}{E_k}\right)[1 - f_s(E_k)] f_n(E_k - eV) , \tag{53}$$

where f_s, f_n are quasiparticle distribution functions for the superconducting and normal sides, and V is the voltage of the normal metal relative to the superconductor. $\epsilon_q = E_k - eV$ is the initial band energy of the hole in the normal side, and conservation of energy is assumed in the tunneling process.

(2) Hole goes from N to S and an excitation of energy E_k is destroyed in S, with probability $|v_k|^2$. Again adding the contributions from two momentum states [v^2 and v'^2 in Eq. (14)],

$$J_{\rm NS}^{(2)} = \left(1 - \frac{\nu}{E_k}\right) f_s(E_k)[1 - f_n(E_k + eV)] . \tag{54}$$

Here, the initial band energy of the hole is $\epsilon_q = -E_k - eV$.

(3) Hole goes from S to N, and destroys an α_k excitation in S:

$$J_{\rm NS}^{(3)} = \left(1 + \frac{\nu}{E_k}\right) f_s(E_k)[1 - f_n(E_k - eV)] . \tag{55}$$

(4) Hole goes from S to N, and creates a β_k excitation in S:

$$J_{\rm NS}^{(4)} = \left(1 - \frac{\nu}{E_k}\right)[1 - f_s(E_k)] f_n(E_k + eV). \tag{56}$$

The net hole current from the normal metal to the superconductor involving quasiparticles of energy E_k is then proportional to

$$J_{\rm NS} = \left(1 + \frac{\nu}{E_k}\right)[f_n(E_k - eV) - f_s(E_k)] + \left(1 - \frac{\nu}{E_k}\right)[f_s(E_k) - f_n(E_k + eV)]. \tag{57}$$

The total current is obtained by integrating over all momentum states of the hole in the superconductor, for which we assume a constant density of states in the normal state. Using the relation

$$d\epsilon_k = \frac{E_k}{a_0 \sqrt{E_k^2 - \Delta_0^2}} dE_k , \tag{58}$$

with a_0 given by Eq. (13d), and assuming the tunneling matrix element is independent of energy and momentum, we obtain for the total current

$$I_{\rm NS} = \frac{1}{eRa_0}\int_{\Delta_0}^{\infty} dE \frac{E}{\sqrt{E^2-\Delta_0^2}}\left[\left(1+\frac{\nu}{E}\right)[f_n(E-eV) - f_s(E)] + \left(1-\frac{\nu}{E}\right)[f_s(E) - f_n(E+eV)]\right] , \quad (59)$$

with R the resistance of the junction when both electrodes are in the normal state. This agrees with the result Eq. (34) for large Z.

Next we consider quasiparticle tunneling between two superconductors separated by an ideal tunnel barrier. The analysis is similar and we omit the details. The net current from superconductor A to B involving quasiparticles of energy E_k in electrode B is now proportional to

$$J_{AB} = \left(1+\frac{\nu_A}{E_k-eV}\right)\left(1+\frac{\nu_B}{E_k}\right) \times[f_A(E_k-eV) - f_B(E_k)] + \left(1-\frac{\nu_A}{E_k+eV}\right)\left(1-\frac{\nu_B}{E_k}\right) \times[f_B(E_k) - f_A(E_k+eV)] \quad (60)$$

and the total current is

$$I_{AB} = \frac{1}{eRa_Aa_B}\int_{-\infty}^{\infty} dE \frac{|E-eV|}{\sqrt{(E-eV)^2-\Delta_{0A}^2}} \times \frac{|E|}{\sqrt{E^2-\Delta_{0B}^2}} + \left(1+\frac{\nu_A}{E-eV}\right)\left(1+\frac{\nu_B}{E}\right) \times[f_A(E-eV) - f_B(E)] , \quad (61)$$

where energies such that $|E| < \Delta_{0B}$ or $|E-eV| < \Delta_{0A}$ are to be excluded from the integral. Equation (61) reduces to Eq. (59) when one of the electrodes is normal. Setting $J_{AB} = 0$ in Eq. (60) yields for small voltage and temperature gradient

$$V = \frac{\nu_A+\nu_B}{e}\frac{T_B-T_A}{(T_A+T_B)/2}\frac{1}{1+\frac{\nu_A\nu_B}{E_k^2}} , \quad (62)$$

which is not independent of E_k as in the NS case. Thus in general the zero current voltage needs to be obtained numerically from Eq. (61). If however either $\nu_A/\Delta_{0A} \ll 1$ or $\nu_B/\Delta_{0B} \ll 1$ (or both) the zero current voltage is approximately given by

$$V_t = \frac{\nu_A+\nu_B}{e}\frac{T_B-T_A}{(T_A+T_B)/2} , \quad (63)$$

so that it is simply the sum of the contributions each electrode would make to the thermoelectric power of a NIS junction, Eq. (44). For a generalized barrier we expect that the asymmetry parameters ν_A and ν_B in Eq. (63) should be replaced by their generalized forms as in Eq. (49). A detailed treatment will be left for future work.

VI. MODEL PARAMETERS

We consider here the various parameters in the model of hole superconductivity used in the previous sections. The microscopic Hamiltonian for the superconductor is assumed to involve on-site, nearest-neighbor, and hopping interactions:

$$H = -\sum_{\substack{\langle ij\rangle \\ \sigma}}[t_{ij} + (\Delta t)_{ij}(n_{i,-\sigma}+n_{j,-\sigma})](c_{i\sigma}^{\dagger}c_{j\sigma} + \text{H.c.}) + U\sum_i n_{i\downarrow}n_{i\uparrow} + \sum_{\langle ij\rangle} V n_i n_j . \quad (64)$$

We define

$$K = 2z\Delta t , \quad (65a)$$

$$W = zV , \quad (65b)$$

with z the number of nearest neighbors, and the reduced interactions

$$u = gU , \quad (66a)$$

$$k = gK , \quad (66b)$$

$$w = gW , \quad (66c)$$

with g the density of states at the Fermi level. For a constant density of states,

$$g = \frac{1}{D} , \quad (67)$$

with D the bandwidth, given by

$$D = D_h + nK , \quad (68)$$

with n the number of holes in the band.

The critical temperature in the weak coupling limit is given by[6,16]

$$T_c = \frac{e^{\gamma}}{\pi}D\sqrt{n(2-n)}e^{-a/b} , \quad (69)$$

with γ Euler's constant (=0.577),

$$a = 1 + 2k(1-n) - w(1-3n+3/2n^2) + (k^2-wu)(1-n)^2 , \quad (70a)$$

$$b = 2k(1-n) - w(1-n)^2 - u + (k^2-wu) \times(1-n+n^2/2) . \quad (70b)$$

The gap parameter c [Eq. (6)] is found to be

$$c = \frac{k+(1-n)[k^2-w(1+u)]}{(k^2-wu)a/b-w} - (1-n) , \quad (71)$$

independent of temperature in this regime. For a constant density of states, $1-n = -\mu/(D/2)$. Using Eqs.

(6), (13), and (71) we find for the gap slope

$$\frac{\delta}{\sqrt{1+\delta^2}} = \frac{k+(1-n)[k^2-w(1+u)]}{b}\frac{\Delta_0}{D/2} \tag{72}$$

and the parameter ν follows from Eq. (13c). This implies in particular that the relation

$$\frac{\nu(T)}{\nu(0)} = \frac{\Delta_0^2(T)}{\Delta_0^2(0)} \tag{73}$$

holds in the weak coupling regime. The zero temperature gap obeys the BCS relation

$$\frac{2\Delta_0}{k_B T_c} = 3.53 \tag{74}$$

and the gap near T_c also follows the usual BCS behavior[17]

$$\frac{\Delta_0(T)}{\Delta_0(0)} = 1.74\left(1-\frac{T}{T_c}\right)^{1/2} . \tag{75}$$

Thus we can extract the zero temperature value of ν from the slope of $\nu(T)$ near T_c:

$$\nu(0) = 0.330\frac{\nu(T)}{1-T/T_c} . \tag{76}$$

As discussed in the previous section the thermoelectric effect for nonideal tunnel barriers will give information on $\nu(T)$ near $T = T_c$ but not at temperatures much smaller than T_c. Equation (72) also implies that the gap slope δ approaches zero as $T \to T_c$.

The gap slope δ can be nonzero even in the absence of hopping interaction ($\Delta t = 0$). In the usual extended Hubbard model superconductivity can arise if u or w is negative.[16] The gap slope for $\Delta t = 0$ is

$$\frac{\delta}{\sqrt{1+\delta^2}} = \frac{-w(1+u)(1-n)}{b}\frac{\Delta_0}{D/2} . \tag{77}$$

For a half-filled band ($n = 1$) δ vanishes. This is to be expected because the model is electron-hole symmetric. For $n \neq 1$ however a nonzero gap slope and hence a thermoelectric effect will in general exist even though the Hamiltonian is electron-hole symmetric, because the occupation breaks electron-hole symmetry. For on-site repulsion and nearest-neighbor attraction ($u > 0$, $w < 0$) δ is positive for $n < 1$ and negative for $n > 1$. Physically this implies that the thermoelectric effect will have the same sign as the carriers in the normal state: positive if they are holes, negative if they are electrons. If $w > 0$ and $u < 0$ however the sign of δ is reversed, provided $|u| < 1$. That is, for on-site attraction and nearest-neighbor repulsion the predicted thermoelectric effect is negative for hole carriers and positive for electron carriers.

Assuming the more plausible physical situation where both u and w are positive however, superconductivity will arise from the Hamiltonian Eq. (64) only if the hopping interaction [Eq. (66b)] $k \neq 0$, and $k > 0$ is the appropiate sign expected to occur in nature.[7] For realistic interaction parameters in this model superconductivity occurs only for low hole concentration ($n < 0.2$).[6] In the limit $n \to 0$

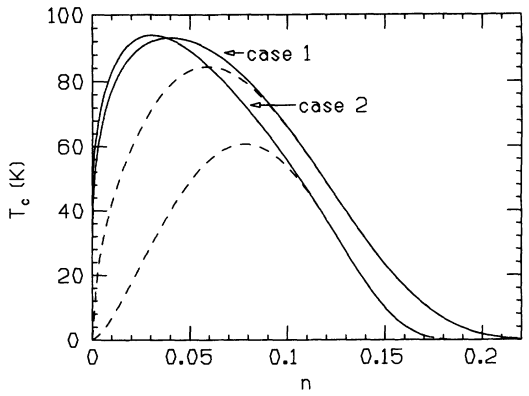

FIG. 14. Critical temperature versus hole concentration for parameters corresponding to case 1 and case 2; the maximum T_c for parameters of case 1 occurs at a somewhat higher hole concentration. The dashed lines give the results from the weak coupling formula Eq. (56).

the gap slope can be written as

$$\frac{\delta}{\sqrt{1+\delta^2}} = \frac{b+u-k}{b}\frac{\Delta_0}{D/2} . \tag{78}$$

To have $T_c > 0$ it is required that $b > 0$. Furthermore $u > k$ is expected for realistic parameters. This also follows from the stability conditions[18,19]

$$k < \frac{u+w}{2} , \tag{79a}$$

$$w < u . \tag{79b}$$

This implies that the gap slope Eq. (78) is positive. In the entire range of n where T_c is nonzero it is found that the gap slope is positive for physical parameters.

The critical temperature for the two sets of interaction parameters used in the previous section is plotted versus hole concentration in Fig. 14. We also show the results from the weak coupling formula Eq. (69), which join the numerical results at large hole concentration as the system enters the weak coupling regime.[20] Figure 15

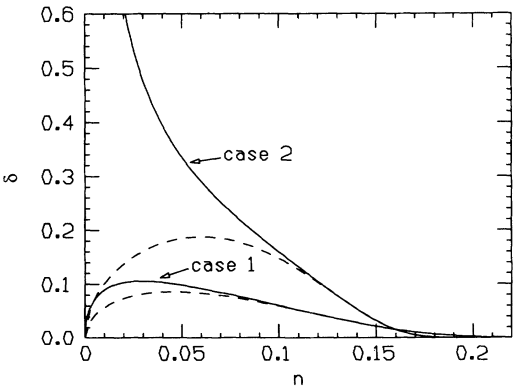

FIG. 15. Gap slope δ versus hole concentration for parameters of case 1 and case 2. The larger gap slope corresponds to case 2. The dashed lines give the results of the weak coupling formula Eq. (59).

shows the gap slope versus hole concentration for these two cases together with the weak coupling results.

VII. CONCLUSIONS

We have studied the crossover between a metallic contact and a tunnel junction between a normal metal and a superconductor for the case where the superconductor has an energy-dependent gap function. Although we have assumed the simple linear energy dependence that arises in the model of hole superconductivity, our analysis should apply approximately to any nonconstant gap function with nonzero slope at the chemical potential. The finite gap slope causes an imbalance in the electron and hole branch occupations in the superconductor; as a result, quasiparticles have a nonzero charge on the average. For the sign of the gap slope predicted in the model of hole superconductivity the sign of this charge is positive.

The probability currents were found to differ from the electron-hole symmetric (EHS) case studied by Blonder *et al.* in the following ways: (i) The ordinary reflection, as well as transmission probabilities, is different for incident electrons and holes of the same energy, and (ii) the probability of Andreev reflection is strongly suppressed even in the limit of vanishing barrier strength. The Andreev reflection probability however was found to be symmetric for electrons and holes.

Correspondingly, the tunneling characteristics differ from the EHS case in the following ways: (i) An asymmetry exists for a wide range of barrer strengths, as found earlier in the ideal tunnel barrier case,[8] and (ii) the low voltage conductance can be strongly suppressed even in the limit of vanishing barrier strength. In the EHS case instead the low voltage conductance is twice the high voltage conductance for vanishing barrier strength. The results for our case cannot be represented by an "effective barrier strength"[5] in the EHS case: For example, a situation where the low voltage conductance is suppressed but no enhanced conductance exists at voltages somewhat above the superconducting gap is never seen in the EHS case. It should be noted that it is frequently seen in tunneling into high-T_c oxide superconductors that a decreased low voltage conductance can exist without accompanying conductance peaks at higher voltages.

The main purpose of this study was to examine the dependence of the thermoelectric effect predicted in the ideal tunnel barrier case for a more general barrier. As the strength of the barrier decreases it was found that the strength of the effect in general decreases. In particular the open circuit thermoelectric voltage was found to vanish for any nonideal barrier as the temperature is lowered sufficiently below T_c. The dependence on barrier strength becomes weaker as the temperature increases, and in particular very close to T_c the effect can even be larger for a nonideal barrier than for an ideal one. These results indicate that the effect will be observable for a wider class of tunnel barriers for temperatures close to T_c.

We also discussed the dependence of the gap slope and hence the thermoelectric effect on microscopic Hamiltonian parameters for a general tight-binding model in the weak coupling regime. It was found that even in the presence of only on-site and nearest-neighbor density-density interactions (extended Hubbard model) the gap slope will be nonzero in general, so that a thermoelectric effect is expected (unless the band is exactly half-filled or there is only an on-site interaction). However, it is only in the model of hole superconductivity, where superconductivity is induced by the off-diagonal hopping interaction Δt, that the sign of the gap slope and hence of the resulting thermoelectric effect is expected to be universal.

Experimental observation of a thermoelectric effect in a NIS tunnel junction was reported by Smith *et al.*,[10] and was attributed to the energy dependence of the electron tunneling probability across the barrier. However, both in the continuum model of Blonder *et al.* and in the tight-binding models considered in this paper (previous sections and Appendix B) no thermoelectric effect would arise in the absence of electron-hole symmetry breaking in the electrodes themselves. The sign of the effect reported by Smith *et al.* (negative thermopower) is opposite to what is predicted by the model of hole superconductivity. Also Clarke and Freake[11] reported measurement of a thermoelectric effect in a Pb-Pb point-contact junction of opposite sign to what is predicted here. The reason for this discrepancy is unclear (although the alternative model for the barrier discussed in Appendix B would appear to predict an asymmetry of the reported sign, we do not believe that model to be relevant to the real situations). On the other hand Kartsovnik *et al.*[21] reported observation of a thermoelectric effect across a SNS Ta-Cu-Ta junction with sign in agreement to what is predicted here.

Current experimental capabilities should allow for observation of this thermoelectric effect for a wide range of superconductors. We hope that such experiments will be undertaken, as they would provide fundamental information on the nature of the superconducting state. As seen from the results in this paper it should be kept in mind that the absence of an effect for temperatures much lower than T_c could be due to nonideal tunnel barriers rather than being intrinsic. A particularly interesting setup may be scanning tunneling spectroscopy in vacuum, as it may allow for the existence of large temperature gradients across the gap; in that setup the crossover between tunnel junction and metallic contact discussed here would be achieved as the distance between tip and sample is decreased.[22]

There is another aspect related to the thermoelectric effect that should be mentioned. When a current circulates across a tunnel barrier a temperature difference should develop across the junction, proportional to the thermopower (Peltier effect). If the thermopower is positive as expected, the negatively biased electrode will become hotter. In particular this will tend to counteract the asymmetry expected in tunneling characteristics: When the superconductor is negatively biased, where a larger dI/dV is expected, its temperature will increase when current circulates and this will tend to suppress the peak in dI/dV. Conversely when the superconductor is pos-

itively biased its temperature will decrease and dI/dV increase. The importance of this effect will depend on the electrical and thermal conductivities of the junction.

The thermoelectric effect in tunnel junctions could also have practical applications. Usually thermoelectric effects in metals and semiconductors become smaller as the temperature is lowered, in contrast to the effect discussed here. Furthermore the effect considered here will be sensitive to the application of magnetic fields and could be turned on and off that way. Possible device applications may be in thermometry, as the effect may provide an accurate way to measure temperature and temperature differences at low temperatures, and in bolometry, as a sensitive detection device for radiation incident on one side of the junction. Another application could arise from the Peltier effect discussed above: A tunnel junction or an array of such junctions with one or both electrodes superconducting may serve as a small refrigeration unit at low temperatures, where other methods may be less efficient. The possibility of using superconducting tunnel junctions in refrigeration has been discussed before.[23] A practical challenge for these applications will be to construct tunnel junctions of finite electrical conductivity but sufficiently low thermal conductivity.

ACKNOWLEDGMENT

This work was supported by the Department of Physics, University of California, San Diego.

APPENDIX A

We list here some useful relations involving the coherence factors Eq. (14). These relations are valid in the energy range $\Delta_0 < E < \Delta_0^2/\nu$. For $E > \Delta_0^2/\nu$ the relations are valid with v on the left-hand side replaced by $(-v)$. Some frequently appearing combinations are

$$uu' + vv' = \frac{\Delta_0}{E} , \tag{A1a}$$

$$uu' - vv' = \frac{\nu}{\Delta_0} , \tag{A1b}$$

$$uv' + u'v = \frac{1}{a_0} , \tag{A1c}$$

$$uv' - u'v = \frac{\sqrt{E^2 - \Delta_0^2}}{E} . \tag{A1d}$$

Other useful relations are

$$u^2 - v^2 = \frac{\sqrt{E^2 - \Delta_0^2}}{a_0 E} + \frac{\nu}{E} , \tag{A2a}$$

$$v'^2 - u'^2 = \frac{\sqrt{E^2 - \Delta_0^2}}{a_0 E} - \frac{\nu}{E} , \tag{A2b}$$

$$uv = \frac{1}{2a_0 E}(\Delta_0 - \delta\sqrt{E^2 - \Delta_0^2}) , \tag{A2c}$$

$$u'v' = \frac{1}{2a_0 E}(\Delta_0 + \delta\sqrt{E^2 - \Delta_0^2}) , \tag{A2d}$$

$$u^2 + v^2 = u'^2 + v'^2 = 1 . \tag{A2e}$$

APPENDIX B: AN ALTERNATIVE MODEL FOR THE BARRIER

An alternative way to describe the generalized barrier is to assume a different on-site energy for the boundary site. This is the discrete analog of the continuum model considered by Blonder *et al.* The noninteracting Hamiltonian is, instead of Eq. (1),

$$H_0 = -t\sum_{i\sigma}(c_{i\sigma}^\dagger c_{i-1,\sigma} + \text{H.c.}) + \epsilon_0 \sum_\sigma c_{0\sigma}^\dagger c_{0\sigma} - \mu \sum_{i\sigma} c_{i\sigma}^\dagger c_{i\sigma} . \tag{B1}$$

Solution of the Bogoliubov equations at the boundary yields for the wave function amplitudes

$$a = \left[vv' + \frac{\delta}{2}(uv' + u'v) + ir\frac{\delta}{2}(uv' - u'v)\right] \Big/ \gamma , \tag{B2a}$$

$$b = -\left[\left\{Z^2 + iZ + \frac{\delta^2}{4}(1 + r^2)\right\}[uv' - u'v] + \frac{\delta}{2}(2iZ - ir - 1)(uu' + u'v)\right] \Big/ \gamma , \tag{B2b}$$

$$c = \left[(1 - iZ)v' + \frac{\delta}{2}(1 - ir)u'\right] \Big/ \gamma , \tag{B2c}$$

$$d = \left[iZv + \frac{\delta}{2}(1 + ir)u\right] \Big/ \gamma , \tag{B2d}$$

$$\gamma = uv' + \left(Z^2 + \frac{\delta^2}{4}(1 + r^2)\right)(uv' - u'v) + \frac{\delta}{2}(uu' - vv') + i\frac{\delta}{2}(2Z - r)(uu' + vv') . \tag{B2e}$$

Here the barrier strength is given by

$$Z = \frac{\epsilon_0}{2t \sin k_F} = \frac{\epsilon_0}{v_F} , \tag{B3}$$

similarly to Blonder *et al.* (v_F is the Fermi velocity). For $\delta = 0$ Eq. (B2) coincides with the results of Blonder *et al.* The parameter r is given by

$$r = \frac{\cos k_F}{\sin k_F} + \frac{2(\Delta_{00} - \Delta_{00}')}{v_F \delta} . \tag{B4}$$

Here, Δ'_{00} is the on-site gap component at the boundary site, which could be different from its bulk value Δ_{00}. In the treatment of Blonder *et al.* it was assumed that $\Delta'_{00} = \Delta_{00}$.

In the absence of electron-hole asymmetry the tunneling characteristics predicted by this barrier go over to the ideal tunnel barrier result for any value of Δ'_{00} as $Z \to \infty$. However, when electron-hole asymmetry exists the situation is more subtle: The reflection coefficient for incident holes in the large Z limit is found to be

$$B = 1 - \frac{a_0}{Z^2} \frac{E}{\sqrt{E^2 - \Delta_0^2}} \left[1 - \frac{\nu}{E}\left(1 + \frac{r}{Z}\right)\right] \qquad \text{(B5)}$$

instead of Eq. (33). If we assume $\Delta'_{00} = \Delta_{00}$ we find in taking the limit $Z \to \infty$ that the tunneling asymmetry obtained is of the same magnitude as in the ideal tunnel barrier case *but with the sign reversed.* The correct sign and magnitude of the tunneling asymmetry is obtained if we assume that as $Z \to \infty$, $(\Delta_{00} - \Delta'_{00}) \to -\delta(\epsilon_0 - \epsilon_F/2)$, with $\epsilon_F = -2t\cos k_F$ the Fermi energy. We have not been able to verify from self-consistent solution of the Bogoliubov equations whether this is indeed the case.

The difficulty with this kind of barrier arises because it introduces an additional electron-hole asymmetry beyond the one assumed in the superconducting electrode. However, it would seem that the type of barrier treated in the bulk of this paper is a more realistic representation of what occurs in a real experimental situation. It should also be noted that even for the type of barrier discussed here no asymmetry in tunneling or a thermoelectric effect would arise if the gap function in the superconductor has no energy dependence.

[1] L. Solymar, *Superconductive Tunneling and Applications,* (Chapman and Hall Ltd, London, 1972), and references therein.

[2] M. Tinkham, Phys. Rev. B **6**, 1747 (1972).

[3] M.H. Cohen, L.M. Falicov, and J.C. Phillips, Phys. Rev. Lett. **8**, 316 (1962).

[4] G.E. Blonder, M. Tinkham, and T.M. Klapwijk, Phys. Rev. B **25**, 4515 (1982).

[5] G.E. Blonder and M. Tinkham, Phys. Rev. B **27**, 112 (1983).

[6] J.E. Hirsch and F. Marsiglio, Phys. Rev. B **39**, 11515 (1989); Physica C **162–164**, 591 (1989); F. Marsiglio and J.E. Hirsch, Phys. Rev. B **41**, 6435 (1990).

[7] J.E. Hirsch, Physica C **158**, 326 (1989); Phys. Rev. B **48**, 3327 (1993).

[8] F. Marsiglio and J.E. Hirsch, Physica C **159**, 157 (1989).

[9] *Nonequilibrium Superconductivity,* edited by D.N. Langenberg and A.I. Larkin (North-Holland, Amsterdam, 1986), and references therein.

[10] A.D. Smith, M. Tinkham, and W.J. Skocpol, Phys. Rev. B **22**, 4326 (1980).

[11] J. Clarke and S.M. Freake, Phys. Rev. Lett. **29**, 588 (1972).

[12] J.E. Hirsch, Phys. Rev. Lett. **72**, 558 (1994).

[13] P.G. de Gennes, *Superconductivity of Metals and Alloys* (Benjamin, New York, 1966), Chap. 5.

[14] J.E. Hirsch, Physica C **194**, 119 (1992).

[15] The constant $\frac{1}{a_0}$ was inadvertently omitted from the expression for the current in Ref. 12.

[16] R. Micnas, J. Ranninger, and S. Robaszkiewicz, Phys. Rev. B **39**, 11653 (1989).

[17] G. Rickayzen, in *Superconductivity,* edited by R.D. Parks (Dekker, New York, 1969), Vol. 1, p. 51.

[18] J.E. Hirsch and F. Marsiglio, Phys. Lett. A **140**, 122 (1989).

[19] D.C. Mattis, Int. J. Mod. Phys. B **3**, 389 (1989).

[20] F. Marsiglio and J.E. Hirsch, Physica C **165**, 71 (1989).

[21] M. V. Kartsovnik, V.V. Ryazanov, and V.V. Shmidt, JETP Lett. **33**, 356 (1981).

[22] T. Hasegawa, M. Nantoh, and K. Kitazawa, Jpn. J. Appl. Phys. **30**, L276 (1991).

[23] R.G. Melton, J.L. Paterson, and S.B. Kaplan, Phys. Rev. B **21**, 1858 (1980).